Fusion Engineering and Design 135 (2018) 314–323

Contents lists available at ScienceDirect

Fusion Engineering and Design

journal homepage: www.elsevier.com/locate/fusengdes

MHD thermohydraulics analysis and supporting R&D for DCLL blanket in the FNSF

Sergey Smolentsev[a,*], Tyler Rhodes[a], Gautam Pulugundla[a], Cyril Courtessole[a], Mohamed Abdou[a], Siegfried Malang[b], Mark Tillack[c], Chuck Kessel[d]

[a] University of California Los Angeles, USA
[b] Independent consultant, Germany
[c] University of California San Diego, USA
[d] Princeton Plasma Physics Laboratory, USA

ARTICLE INFO

Article history:
Received 18 January 2017
Received in revised form 11 June 2017
Accepted 11 June 2017
Available online 16 June 2017

Keywords:
Blanket
Lead-lithium
DCLL
FNSF
Magnetohydrodynamics
Pressure drop

ABSTRACT

A Fusion Nuclear Science Facility (FNSF) has been recognized in the fusion community as a necessary facility to resolve the critical technology issues of in-vessel components prior to the construction of a DEMO reactor (Abdou et al., 1996) [1]. Among these components, development of a reliable, low-cost and safe blanket system that provides self-sufficient tritium breeding and efficient conversion of the extracted fusion energy to electricity, while meeting all material, design and configuration limitations is among the most important but still challenging goals. In the recent FNSF study in the US (Kesel et al., 2015) [2], a Dual-Coolant Lead-Lithium (DCLL) blanket has been selected as the main breeding blanket concept. This paper summarizes the most important details of the proposed DCLL blanket design, presents the MHD thermohydraulic analysis for the PbLi flows in the blanket conduits and introduces supporting R&D studies, which are presently ongoing at UCLA. We also discuss the required pre-FNSF R&D in the area of MHD Thermofluids to support the further work on the DCLL blanket design & analysis and its integration into the fusion facility.

1. Introduction

The DCLL is an attractive breeding blanket concept that potentially leads to a high-temperature ($T \sim 700\,^{\circ}C$), high thermal efficiency ($\eta > 40\%$) blanket system. In this concept, a high-temperature lead-lithium (PbLi) alloy circulates slowly ($U \sim 10$ cm/s) in large poloidal rectangular ducts ($D \sim 20$ cm) to remove the volumetric heat generated by neutrons and produce tritium, while a pressurized (typically to 8 MPa) helium gas (He) is used to remove the surface heat flux and to cool the ferritic first wall (FW) and other blanket structures in the self-cooled region. The key element of the concept is a flow channel insert (FCI) that serves as an electrical or electrical/thermal insulator to reduce the magnetohydrodynamic (MHD) pressure drop and to decouple the temperature-limited RAFM (reduced-activation ferritic/martensitic) steel wall from the flowing hot PbLi.

Several designs of the DCLL blanket have been proposed in Europe [3–6], the US [7–11] and China [12–14]. At present, a module-type DCLL blanket is considered in Europe for a possible implementation in a DEMO reactor [15]. Historically, the first DCLL version, known as a low-temperature (LT) DCLL blanket [3], relied on qualified materials and existing fabrication technologies. A key component of this design is a sandwich-type FCI composed of steel/alumina/steel layers or a thin alumina layer placed on the wall to be used as electrical insulator for decoupling electrically conducting structural walls from the flowing PbLi. In the next, more advanced high-temperature (HT) DCLL blanket, which was first introduced in [8], an FCI made of silicon carbide (SiC), either composite [16] or foam [17], was further proposed as a means for electrical and also thermal insulation to provide acceptable MHD pressure drops and to achieve a high PbLi exit temperature. At present, the LT DCLL with a sandwich FCI is considered in the fusion community as a backup option in case a SiC FCI could not be developed and fully qualified prior to the start-up of the FNSF. More information about the DCLL blanket developments, blanket key features and technical characteristics as well as several design examples can be found in [18].

In the recent FNSF study in the US [2], a DCLL blanket was designed for both inboard and outboard regions (Fig. 1). The entire machine is subdivided into 16 toroidal sectors, such that there are

* Corresponding author.
E-mail address: sergey@fusion.ucla.edu (S. Smolentsev).

https://doi.org/10.1016/j.fusengdes.2017.06.017
0920-3796/

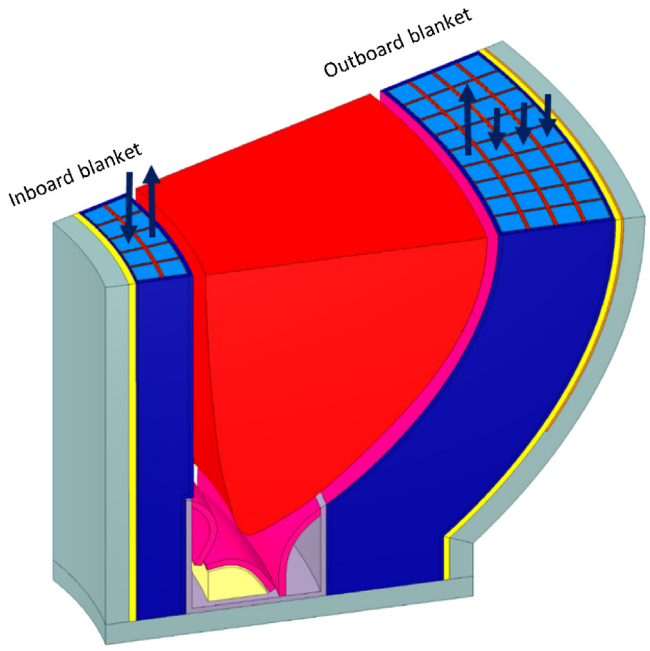

Fig. 1. Cross-cut of one of the 16 toroidal sectors in the FNSF with the IB and OB blankets. The arrows show the PbLi flow path in the poloidal ducts.

16 inboard (IB) and 16 outboard (OB) blankets. Each sector with the blankets can be removed via an individual port using a horizontal maintenance scheme. In the IB blanket, the liquid metal flows upwards in the five front ducts facing the plasma, makes a U-turn at the top of the blanket and then flows downwards in the five rear ducts. There are two manifolds at the bottom of the blanket to feed the poloidal ducts and to collect the hot PbLi at the exit of the blanket. The OB blanket has a similar structure but the number of the ducts and blanket dimensions are different to fit into a larger space at the OB. In the designed blanket, the liquid first flows upwards in the front nine ducts and then downwards through the three rows of return ducts (totally, $3 \times 9 = 27$ return ducts). The thickness of the inboard blanket (including the front wall, back wall, stiffening plates, FCI, He flows and PbLi flows) is 0.5 m. The thickness of the OB blanket is 1 m. The poloidal length of the IB blanket is ~7 m, while the OB blanket is ~ 10 m. The characteristic magnetic field at the IB is ~ 10 T and that at the OB is ~ 5.5 T. Each poloidal blanket duct has a 5-mm thick FCI. The FCI is separated from the RAFM wall with a thin 2-mm gap to accommodate possible thermal expansions of the flow insert. The space inside the FCI box and that in the gap is filled with the flowing PbLi. The most important blanket parameters in this design for two blanket version, LT and HT DCLL, are summarized in Table 1.

In this study, a conservative variant of the HT blanket is considered, where the maximum PbLi temperature is restricted to 550 °C. This temperature choice gives a conservative match to the RAFM steel limits and a reasonably large temperature window. The last parameter in Table 1, the fraction of volumetric heat absorbed by the flowing PbLi, was estimated using a simplified thermal analysis under the assumption that the volumetric heat generated in the FCI and the 2-mm PbLi gap goes to He. A full 3D analysis may find different.

2. MHD thermohydraulics analysis

The goal of this analysis is to evaluate the MHD pressure drop for each blanket component and to eventually calculate the overall pressure drop for the entire blanket through the summation of the individual pressure drop contributions. Similar to the MHD analysis for the IB DCLL DEMO blanket in [19], in this study we identified and then computed five major pressure drops. These five main components of the PbLi loop, which are expected to have the greatest impact on the MHD pressure drop are the following (Fig. 2): (1) flows in the poloidal blanket ducts with FCI; (2) flows at the blanket inlet and outlet (i.e. manifolds); (3) flows in the PbLi access pipes with FCI in a near-uniform magnetic field region; (4) flows in the access pipes in the fringing magnetic field; and (5) flows at the top of the blanket ("U-turn") where changes in the flow direction and flow redistribution occur.

Table 1
The most important blanket parameters used in the present MHD thermohydraulic analysis.

PARAMETER	IB BLANKET	OB BLANKET
Blanket length, m	7.04	10.28
Toroidal length of the FW per sector, m	1.69	2.28
Characteristic B-field, T	10.0	5.5
NWL (averaged), MW/m^2	0.86	1.34
Neutron multiplication in PbLi	1.15	1.15
PbLi Inlet/Outlet T, °C	350/550 (HT DCLL) 350/470 (LT DCLL)	350/550 (HT DCLL) 350/470 (LT DCLL)
FCI thickness, mm	5 (HT DCLL) 3 RAFM+1.5 Alumina + 0.5 RAFM (LT DCLL)	5 (HT DCLL) 3 RAFM+1.5 Alumina + 0.5 RAFM (LT DCLL)
Fraction of volumetric heat absorbed by PbLi	0.78	0.78

In the long poloidal ducts, the MHD pressure drop originates from the nearly fully developed flows where the flow opposing electromagnetic forces arise from the interaction between the induced cross-sectional currents closing in the toroidal-radial plane and the strong plasma-confining toroidal magnetic field. These currents can significantly be reduced by the insulating FCI compared to a flow in a fully conducting duct without an FCI. To serve well its insulating functions, the FCI has to have sufficiently low electrical and thermal conductivity. The requirements on SiC materials for the DCLL blanket under conditions of ITER TBM and DCLL DEMO were formulated in [19,26]. For a 5-mm FCI, the goal was to provide low thermal conductivity of 1–2 W/m-K and electrical conductivity of about 1 S/m for inboard blankets. Higher electrical conductivities of about 50 S/m were found to be sufficient in lower magnetic field outboard blankets.

The degree of the pressure drop reduction is the highest (a few orders of magnitude [19]) when a low-conductivity SiC FCI is used. The sandwich FCI utilized in the present LT DCLL design (Fig. 3) is less effective as an electrical insulator because the induced electric current from the bulk flow can close through a thin 0.5 mm RAFM liner. Correspondingly, the pressure drop reduction by a sandwich FCI is significantly lower compared to the SiC FCI. The difference can especially be important for IB blankets for which the magnetic field is about two times higher. In the present study, the MHD pressure drop in the poloidal flows with the FCI, SiC or sandwich, was computed with the help of a fully developed flow model and a 2D numerical MHD solver developed in [20]. In these recent computations the electrical conductivity of the SiC FCI was chosen at 10 S/m. This relatively low value is needed to minimize the pressure drop in the IB blanket. For the OB blanket, higher (up to 50 S/m) electrical conductivities seem to be acceptable.

Computed velocity distributions in the poloidal flow with the FCI for the IB blanket are shown in Fig. 4. The PbLi flow in the duct with a sandwich FCI demonstrates very high velocity jets at the two side FCI walls (walls parallel to the applied toroidal magnetic field) (Fig. 4a). The maximum velocity in the jets in the bulk flow is about twenty times higher than the mean bulk velocity, i.e. around 2.5 m/s. In practice, such a jet flow will likely demonstrate instabilities and vortex formation [22] resulting in a turbulent flow regime.

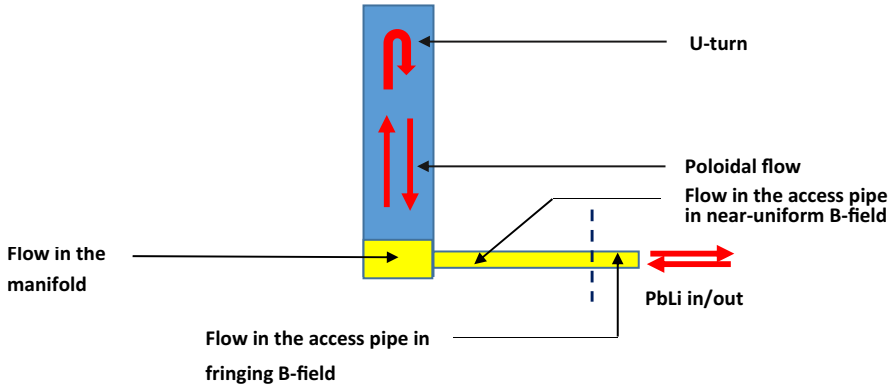

Fig. 2. A simplified sketch of the PbLi flow in the DCLL blanket to identify major MHD pressure drops.

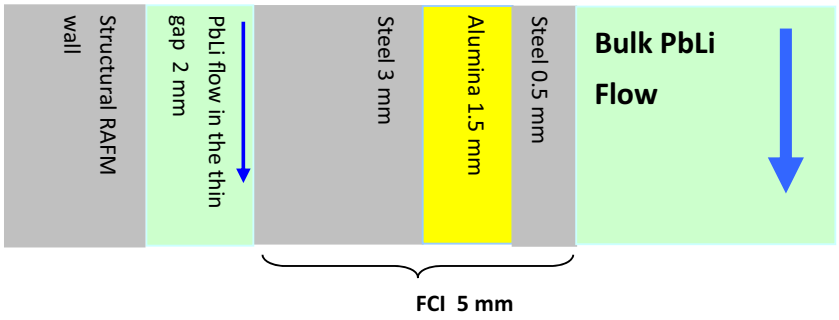

Fig. 3. Structure of the sandwich-type steel/alumina/steel FCI used in the proposed LT DCLL blanket.

The jet instabilities and turbulence would, however, have only a small impact on the pressure loss [23], because the MHD pressure drop in the poloidal flow is mostly controlled by the 2D electric currents closing through the electrically conducting RAFM layer. As seen from Fig. 4c, the PbLi in the thin 2-mm gap between the FCI and the RAFM wall is almost stagnant next to the Hartmann walls (walls perpendicular to the applied toroidal magnetic field), but has a very high velocity (more than ten times higher than the mean bulk velocity) in the side-wall sections of the gap. This velocity distribution may have a strong effect on corrosion, tritium transport and temperature distribution, which are not considered in this study. The velocity distribution in the flow with the SiC FCI is very different (Fig. 4b). Namely, the jet flows are strongly reduced and the flow in the side-wall sections of the gap is comparable with the mean bulk velocity (Fig. 4d). The PbLi in the Hartmann-wall sections of the gap is still stagnant.

The largest contribution into the pressure loss in the blanket is associated with the so-called "3D MHD pressure drop," which is caused by the axial (poloidal) induced electric currents. These currents close their path inside the liquid metal and cannot be reduced by the FCI. The two sources of the highest MHD pressure drop is the 3D MHD flow in the PbLi manifolds and the MHD flow in the radial access pipes in the fringing magnetic field. To calculate these 3D pressure drops, intensive 3D computer modelling was performed in the wide range of the flow parameters and then the computed results were approximated with semi-empirical correlations (for details see Section 3). These correlations were eventually used in the present calculations of the MHD pressure drop.

The MHD flow at the top of the blanket can also demonstrate some 3D features but the associated MHD pressure drop is not high compared to the manifolds and the access pipes because changes in the flow direction occur mostly in the plane perpendicular to the magnetic field, such that the induced axial currents are low compared to the cross-sectional currents. The computed MHD pressure drops are summarized in Table 2. It should be noted that the magnetic field varies over the space occupied by a particular blanket unit within about 1 Tesla. These variations were not taken into account in the present analysis. Instead, a "characteristic" magnetic field was used as shown in Table 1.

It is interesting that the total pressure drop in the OB blanket is more than two times higher compared to the IB blanket even though the magnetic field at the inboard is almost two times higher compared to the outboard. This result is different from other analyses (see e.g. [19]), where the IB pressure drop was found to be higher. This surprising conclusion can be explained by the characteristic features and the operation parameters of the present DCLL blanket design: larger dimensions of the OB blanket and the longer poloidal flow path, and higher neutron heat resulting in higher velocities in all OB blanket components. At the same time, the access pipes in both IB and OB blankets enter the vacuum vessel at about the same location and have about the same length and thus the corresponding flows experience about the same MHD effects.

The computed results in Table 2 for the MHD pressure drop in the blanket have to be evaluated with respect to the maximum allowable pressure in the entire PbLi circuit. In the past (see e.g. BCSS study in the US [24]), the maximum allowable pressure drop in the blanket was considered at 2 MPa. This limit was based on the maximum pumping capacity of one-stage rotary pumps available at that time. At present, the pumping capacity of rotary pumps is significantly higher, suggesting a new pumping limit of about 4 MPa. However, the overall pressure drop in the primary PbLi loop is not limited to only that in the blanket. In fact, the ancillary equipment, including the tritium extraction system, PbLi/He heat exchanger and all PbLi carrying pipes (in addition to those in the blanket) would contribute a large Δp, which is comparable with or can even exceed the MHD pressure drop in the blanket itself. Rough estimates suggest that all individual pressure drops in the ancillary system could sum up to about 2 MPa. This additional pressure drop

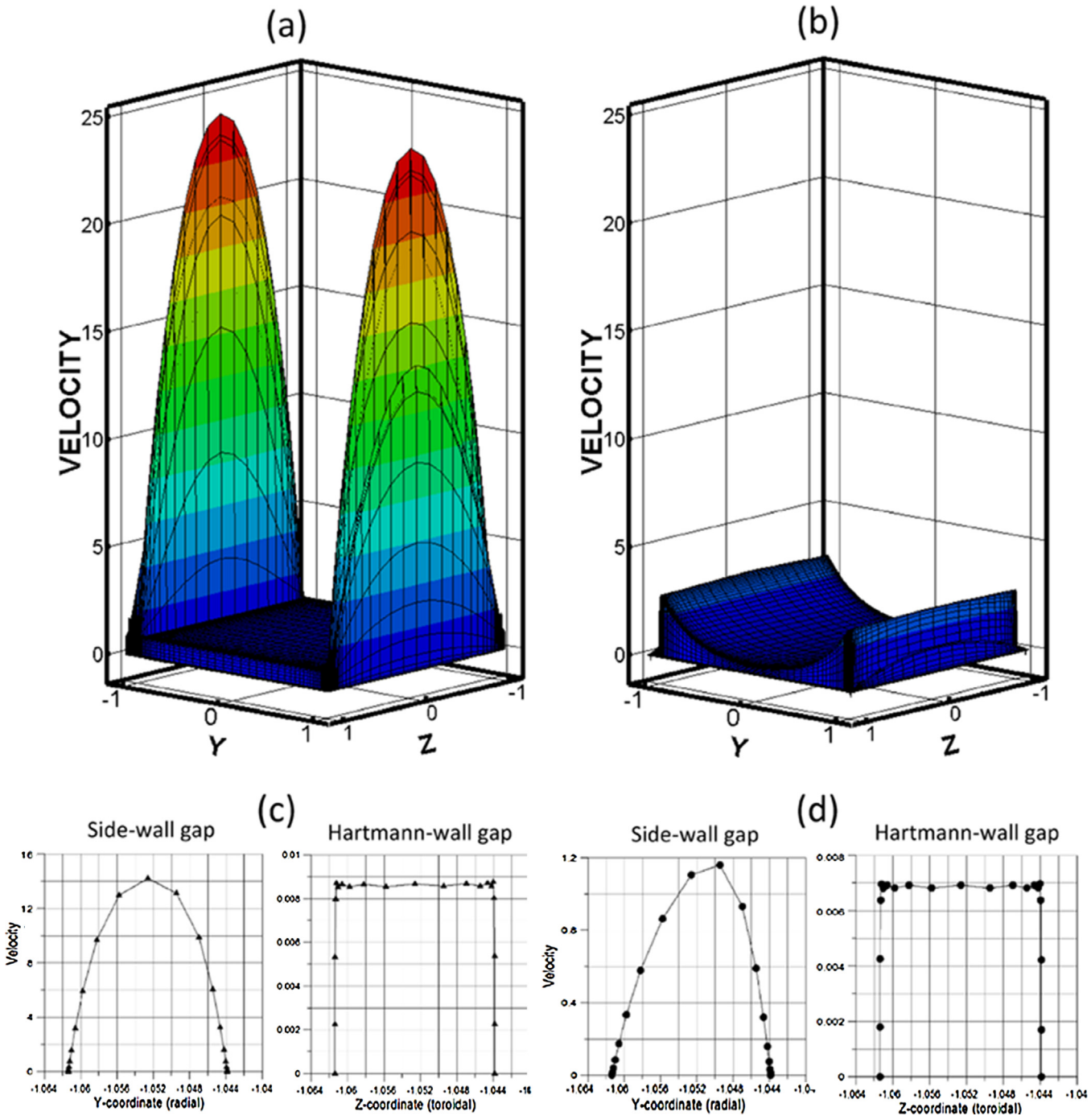

Fig. 4. Velocity distribution in the poloidal flow in the IB blanket. (a) bulk and gap flows, sandwich FCI. (b) bulk and gap flows, SiC FCI. (c) gap flow, sandwich FCI. (d) gap flow, SiC FCI. All velocities are scaled by the mean bulk velocity (see Table III). Magnetic field (toroidal) is in Z direction.

Table 2
Summary of the computed MHD pressure drops.

MHD flow	Δp, MPa in LT DCLL, IB	Δp, MPa in LT DCLL, OB	Δp, MPa in HT DCLL, IB	Δp, MPa in HT DCLL, OB
Poloidal flow with FCI	0.454	0.673	0.017	0.026
Manifold (inlet and outlet)	0.379×2	0.527×2	0.196×2	0.313×2
Access pipe, near-uniform B-field	1.854×2	4.850×2	0.010×2	0.025×2
Access pipe, fringing B-field	0.403×2	1.247×2	0.242×2	0.748×2
Flow redistribution at the top	0.112	0.085	0.067	0.051
TOTAL Δp, MPa	**5.839**	**14.007**	**0.979**	**2.249**

and the maximum pumping capacity of the pump imply a limit on the MHD pressure drop in the blanket (including the access pipes) of about 2 MPa. The present calculations of the MHD pressure drop in the blanket suggest that the HT DCLL will satisfy this limit, while the MHD pressure drop in the LT DCLL is well above. This very high MHD pressure drop in the LT DCLL design originates from higher,

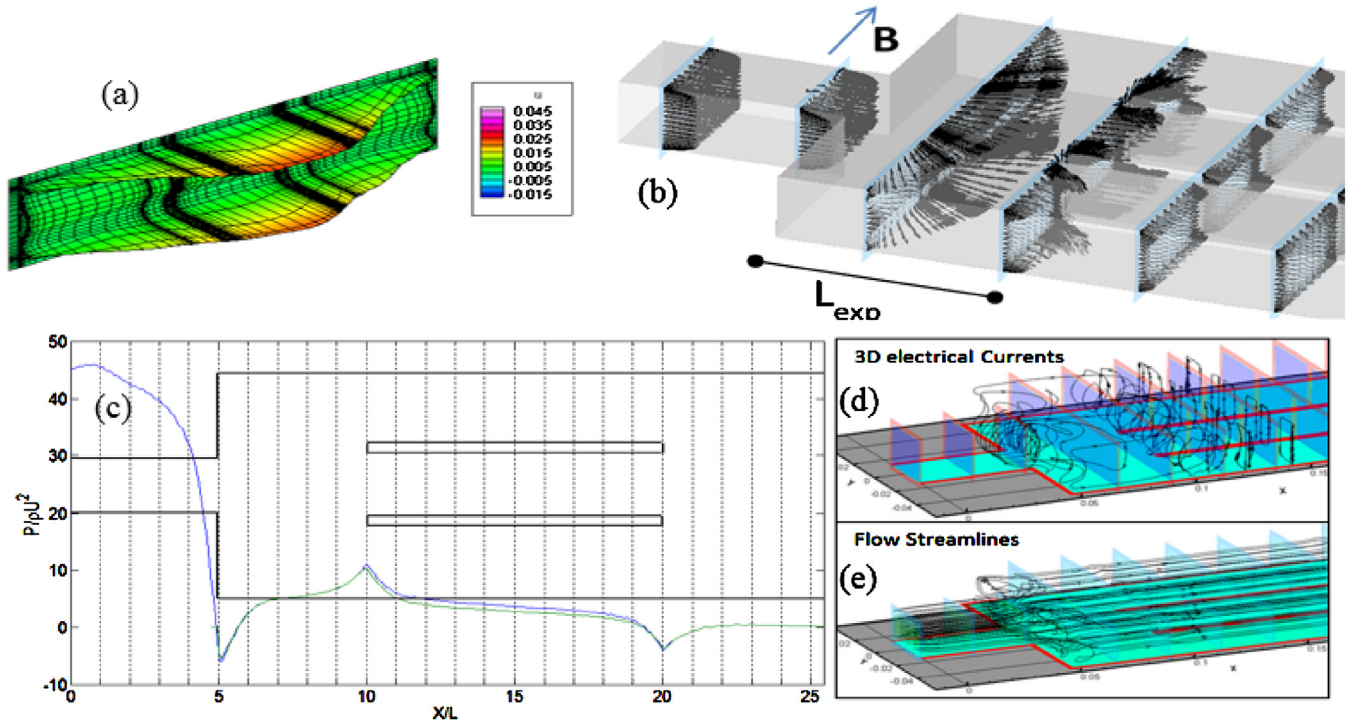

Fig. 5. Results for steady MHD flow through a 3D manifold with non-conducting walls and strong transverse magnetic field at *Ha*=2190 and *Re*=625. (a) Velocity profile in the expansion region. (b) Velocity vectors. (c) Pressure distribution along the centerlines of the channels. (d) Electrical current tracers. (e) Flow tracers.

compared to the HT DCLL, velocities and from the use of a sandwich FCI, which does not provide high enough electrical insulation. This rules out the use of the LT DCLL and the sandwich FCI in the reference fusion facility unless the FNSF operates at much lower power.

Another important consideration is the internal PbLi pressure distribution inside the blanket, which has to be taken into account when doing the stress analysis of the structural and functional (FCI) blanket elements. An additional part of the internal pressure is the static pressure caused by the high density ~9300 kg/m^3 of the fluid, which is almost 1 MPa at the bottom of the 10-m poloidal duct. This may have an important impact on the mechanical stresses in the blanket structure. In the analysis of these stresses, two situations have to be considered, including (1) the normal operation and (2) the accidental internal He-LOCA event that can lead to a pressurization of the entire blanket to the maxim He-pressure of 8 MPa. In the accidental case, the allowable maximum stress is higher compared to the normal operation scenario [25].

To conclude this section, we would like to mention some uncertainties and restrictions of the present analysis. First of all, the fraction of the volumetric heat absorbed by the PbLi flow of 78%, as shown in Table 1, comes from a simplified thermal analysis that does not take into account flow details and, in fact, considers only the volumetric heating and heat diffusion. In this analysis, the thermal conductivity of the SiC FCI was taken at 2 W/m-K to possibly minimize the heat loss from the liquid metal into the cooling He stream. However, taking into account that the temperature difference between the PbLi and the He is not very high compared to a DCLL DEMO blanket, higher thermal conductivities < 10 W/m-K seem to be acceptable. In a more rigorous analysis of the heat loss, this fraction has to be computed as a part of the integrated MHD/heat transfer analysis as it was done in [21] and [26]. Second, the analysis of the MHD pressure drop doesn't include one associated with the current leaking through the junction area between two FCI segments. This could be an additional source of high pressure losses due to 3D MHD effects. Unfortunately, very scarce data for this type of MHD flows are presently available [27]. A number of simplifications were also made in the analysis mostly because the blanket design was not accomplished by the time of the analysis or because of the limited analysis tools. For example, two access pipes with the FCI were considered instead of one co-axial pipe. Also, the MHD pressure drop was computed only for the inlet manifold and that in the outlet manifold was assumed to be the same. These uncertainties and limitations should be mitigated in a next, more detailed analysis.

3. 3D MHD flows in the DCLL blanket

As seen from the MHD thermohydraulic analysis in Section 2 for the reference DCLL blanket, the MHD flow in the manifolds and that in the access pipes are the two major contributors into the pressure loss. Such 3D MHD flows are typical examples of situations where the flow dynamics and the pressure distribution are fully controlled by the 3D MHD effects associated with the induced axial currents, whose path is closed in the liquid. At present, in the blanket design and analysis, such 3D MHD pressure drops are calculated using semi-empirical correlations (see e.g. [28]):

$$\Delta p_{3D} = \xi \frac{\rho U^2}{2}, \tag{1}$$

where ξ is the local pressure drop coefficient. The experimental data suggest $\xi = kN$, where k is the empirical coefficient that depends strongly on the flow geometry and N is the interaction parameter (for definition of N see Section 3.1). Typically, $0.25 < k < 2$ [28]. The accuracy of such correlations is often very low because the selection of k is to some degree arbitrary due to the lack of the experimental or numerical data. In what follows, we present first results of the ongoing 3D numerical studies at UCLA for MHD flows in the blanket inlet manifold in a uniform magnetic field and also results for flows in a circular thin-wall pipe in a fringing magnetic field. These are computed with a 3D MHD unstructured-mesh parallel solver

HIMAG [29]. The results were then used to costruct correlations for the 3D MHD pressure drop.

3.1. Modeling manifold flows

Complex duct geometries, first of all flow distributing and collecting manifolds, are key features of any LM blanket, including the DCLL blanket design. Though these manifolds are small in size compared to the full length of the liquid metal circuit, they can significantly contribute to the total pressure drop of the system. Additionally, the manifolds influence how the flow is distributed among the poloidal channels in the DCLL blanket, which is a primary concern since flow imbalance can lead to unacceptable overheating in underfed channels. Computational studies are currently underway at UCLA, which use HyPerComp/UCLA MHD solver, HIMAG, to solve the full 3D MHD equations on a rectangular collocated mesh in order to simulate the 3D MHD flow through manifolds. Steady state solutions were computed for a range of flow and geometry parameters in order to better understand the physical mechanisms that characterize the 3D pressure drop ΔP_{3D} and flow distribution in order to deduce correlations for ΔP_{3D}. A manifold flow (see Fig. 5) was simulated where liquid metal enters the manifold of height $2a$ through the feeding duct of width $2d$ before entering the expansion region, which has length $L_{\exp}$ and toroidal width $2b$. From the expansion region, the flow proceeds into three or more parallel channels of the width $2h$ each. The flow occurs in a uniform transverse (toroidal) magnetic field B.

The governing equations for the flow in the manifold were solved numerically on non-uniform rectangular meshes. In making each mesh, it was ensured that there are at least 5 nodes inside all Hartmann layers on the walls perpendicular to the magnetic field and 12 nodes inside each side layer on the wall parallel to the magnetic field. Also, higher mesh resolution was used in the liquid next to the back wall of the expansion region, which is perpendicular to the axial direction. Mesh sensitivity study was performed using three meshes: coarse ($110 \times 154 \times 33$), medium ($139 \times 191 \times 40$) and fine ($174 \times 240 \times 50$). Most of the computations were performed using the medium mesh. Fully developed MHD flow is used as the inlet boundary condition in the feeding duct and the outlet boundary condition in the form $\frac{\partial}{\partial x} = 0$ is used at the exit of the manifold. The pressure is set to zero at the outlet and the no slip condition is used at all fluid-wall interfaces. First simulations were started with initially uniform flow conditions. Each simulation was run in parallel on 64 or 128 nodes using a computer cluster until steady state solutions were reached as determined by the L2 norm of the residuals reaching the order of 10^{-10}. The converged solutions were used as initial conditions for subsequent simulations at higher values of the flow parameters to reduce the computational time. The minimal computational time was half a day and the longest simulations ran for a month, depending on the flow parameters. Generally, computational time increased as the Reynolds number was increased.

The reference flow in the manifold flow is fully characterized by the following dimensionless parameters: the Hartmann number, $Ha = bB\sqrt{\sigma/\mu}$; the Reynolds number, $Re = \frac{\rho bU}{\mu}$; the interaction parameter $N = Ha^2/Re$; the expansion ratio, $r_{exp} = b/d$; and the channel size parameter, $s = h/b$. Here, σ is the electrical conductivity, μ is the dynamic viscosity, ρ is the density of the liquid metal, and U is the mean bulk velocity in the expansion region.

The flow distribution in this geometry is controlled by the flow becoming dominantly quasi-two-dimensional in a strong magnetic field (the flow becomes more uniformly distributed in the direction of the applied magnetic field as magnetic field is increased, except for the Hartmann layers) and by the formation of side-layer jets (Fig. 5a), which decay exponentially in the flow direction. As $L_{\exp}$ decreases, a larger portion of the flow will enter the central channel since the jets carry more flow in the center than the sides. The flow distribution becomes more uniform as the Hartmann number or $L_{\exp}$ increases.

The first computations that used the full manifold geometry demonstrated that the largest portion of the total MHD pressure drop comes from the 3D flow at the manifold inlet where the liquid enters the expansion region from the feeding duct (Fig. 5c). Also, the flow distribution was found to be fully controlled by the expansion ratio, and, to much smaller degree by the number of parallel ducts, *i.e.* the effect of the channel size parameter s was found to be negligibly small. That is why in the next computations, in order to study the pressure behavior and flow distribution, sudden expansions were modeled with a range of expansion ratios and flow parameters rather than modeling the full manifold geometry. Mathematical analysis of 2D expansions [30] indicates that when $N >> Ha^{3/2}$, the pressure is dominated by a balance of viscous and electromagnetic forces present in the internal shear layer known as Ludford layer and the 3D MHD pressure drop goes with $\rho U^2 N/Ha^{1/2}$. However, if $N << Ha^{3/2}$, an inertial-electromagnetic force balance dominates instead and the 3D MHD pressure drop goes with $\rho U^2 N^{2/3}$. Until recently, the 3D MHD pressure drops have been widely estimated using the empirical correlations in the form of Eq. (1). While this correlation was useful for obtaining order of magnitude estimations of 3D MHD pressure drop (see *e.g.* [19]), this approach is not very accurate and is not supported by theory. Now, for the first time, formulas for 3D MHD pressure drop have been determined for electrically insulated manifolds that are well supported by the aforementioned analysis of 2D expansions:

$$\Delta P_{3D} = \frac{\rho U^2}{2}\left(k_{ve} N Ha^{-1/2} + d_{ve}\right) \quad \text{for} \quad Ha^{3/2}/\mathrm{N} < 3 \tag{2}$$

$$\Delta P_{3D} = \frac{\rho U^2}{2}\left(k_{ie} N^{2/3} + d_{ie}\right) \quad \text{for} \quad \mathrm{Ha}^{3/2}/\mathrm{N} > 3 \tag{3}$$

Here, k_{ve}, $\mathrm{d_{ve}}$, k_{ie}, and d_{ie} are functions of the expansion ratio, $r_{\exp}$:

$$k_{ve} = 0.31 r_{exp} + 3.08, \tag{4}$$

$$d_{ve} = 342.92 r_{exp} - 1563.85, \tag{5}$$

$$k_{ie} = 0.33 r_{exp} + 1.19, \tag{6}$$

$$d_{ie} = -11.55 {r_{exp}}^2 + 85.43 r_{exp} - 264.39. \tag{7}$$

Equations (2) and (3) together with Eqs. (4)–(7) serve as a pressure model that describes the behavior of the 3D pressure drop in both the viscous-electromagnetic and inertial-electromagnetic regimes. Fig. 6 shows this pressure model plotted against the computed results (for $1000 \le Ha \le 6570$, $50 \le Re \le 2500$ and $4 \le r_{\exp £} 12$) that were used in its making. The RMSE (root-mean-square deviation) and R^2 (coefficient of determination) were also calculated, demonstrating good agreement of the proposed pressure model with the computed results. That would be ideal to compare the obtained correlations with experimental data for MHD pressure drop but such data, to our best knowledge, are not available. Although relevant experiments were performed in the past [31] using a test-section similar to that in Fig. 5c, the measurements in these experiments were limited to the flow distribution in the parallel channels.

3.2. Modeling pipe flows in a fringing magnetic field

Access pipes are typically long (~6-m long in the reference DCLL design) and carry the PbLi of the entire blanket, resulting in PbLi velocities several times higher than in the blanket itself. The most of the flow in the access pipe occurs in a near-uniform magnetic field. The associated pressure drop is small providing the pipe is

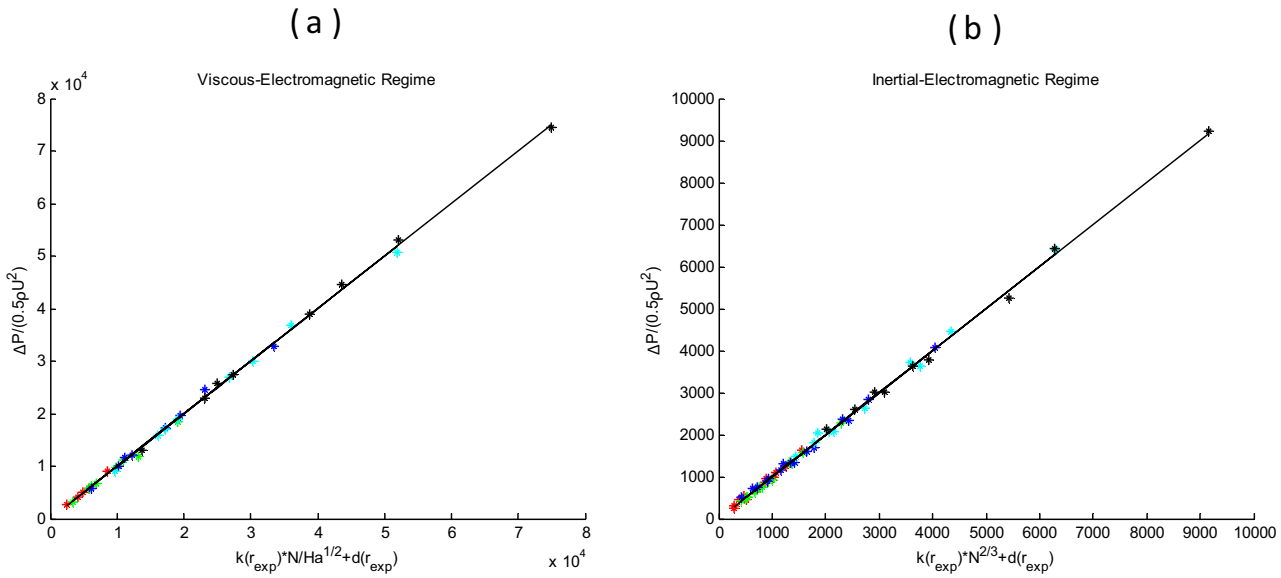

Fig. 6. Proposed pressure model for MHD flows in a non-conducting manifold. (a) In the viscous-electromagnetic regime for $Ha^{3/2}/N < 3$. The RMSE and R^2 for the fit is 540.9 and 0.9989 respectively. (b) In the inertial-EM regime. The RMSE and R^2 is 76.08 and 0.9980 respectively.

well insulated. The 3D part of the MHD pressure drop is related to the flow in a fringing magnetic field, where the access pipe enters the vacuum vessel. It can be significantly higher than the part of the MHD pressure drop associated with the fully developed flow, especially in the case of a non-conducting pipe. Computations for the pipe flows in a fringing magnetic field were performed in [32] in a wide range of the flow parameters *Ha*, *Re*, *N* for several values of the wall conductance ratio, including an insulating pipe. In this study, we approximated the computed data in [32] for the 3D MHD pressure drop in the form of Eq. (1). The numerical value of the coefficient *k* was found to be 0.28, resulting in the following formula for the 3D MHD pressure drop:

$$\Delta p_{3D} = 0.28N\frac{\rho U^2}{2}, \tag{8}$$

where the interaction parameter *N* is built using the pipe radius as the length scale.

4. Pre-FNSF R&D in the area of MHD Thermofluids

The specific R&D topics and research needs related to the use of PbLi as a breeder and coolant were summarized in [27] for a family of DCLL blankets, whereas particular requirements for the DCLL blanket in FNSF were outlined in [33]. The following key research areas have been proposed as follows: (1) LM MHD and heat transfer, (2) MHD corrosion of RAFM steel and deposition of corrosion products, (3) specific effects associated with the use of a flow channel insert, and (4) tritium transport. The near-term R&D studies have to be performed in the existing non-fusion facilities but some relatively large incremental facility upgrades will be needed to extend their capabilities towards new important experiments. As stated in [34], rather than single-effect phenomena, these new experiments should address multiple-effect phenomena, which are critical to the successful development of the DCLL and other LM blanket concepts.

It is important that any proposed experiments in a non-fusion facility prior to FNSF can demonstrate similarity with a real blanket. One approach to ensure such similarity involves utilization of dimensionless parameters that represent ratios between different physical mechanisms or forces acting on the flowing liquid. Such parameters are the hydrodynamic Reynolds number *Re* (ratio of inertia to viscous forces), Hartmann number *Ha* (Hartmann squared is the ratio of electromagnetic to viscous forces), interaction parameter *N* (ratio of electromagnetic to inertia force) and Grashof number *Gr* (approximates ratio of buoyancy to viscous force).

Table 3
Dimensionless parameters *Ha*, *Re*, *Gr* and *N* for the reference DCLL blanket (front duct).

DCLL Blanket	*U*, m/s (in the front duct)	*Ha*	*Re*	*Gr*	*N*
HT IB	0.087	37461	74557	6.59×10^{11}	18822
LT IB	0.144	37461	124260	6.59×10^{11}	11379
HT OB	0.203	15123	174480	1.04×10^{12}	1311
LT OB	0.338	15123	290790	1.04×10^{12}	787

These parameters play a major role in the transfer process in the PbLi MHD flows in the blanket and, therefore, should be used to characterize coupled MHD and heat and mass transfer phenomena. They can also serve as a metrics to measure the R&D progress on the pathway from the present experimental facilities to FNSF and eventually to the DEMO plant. Each blanket component (e.g. manifolds, inlet/outlet pipes, poloidal ducts, etc.) can be characterized with its own sub-set of the parameters. In this study, a set of the parameters was evaluated for the flows in the front poloidal ducts for both IB and OB blankets (see Table 3) and then compared with the same parameters in other blanket concepts and designs using the so-called Ha-Re and Ha-Gr diagrams [35] as shown in Fig. 7. As seen from the figure, the reference DCLL blankets are not very different from other LM blankets. Namely, the MHD flows could be expected in the regime of quasi-two-dimensional (Q2D) turbulence with high impact from buoyancy forces, which are difficult to simulate numerically with the modern MHD computational tools.

As proposed in [33] and also discussed in [34], the near-term R&D studies for the DCLL blanket have to be performed in the existing non-fusion facilities over the period of about10 years starting from now. At the end of this period, a larger step should be taken towards a new experimental blanket facility that will extend MHD thermofluid studies to more integrated tests at higher operation parameters for more prototypic configurations including full-scale blanket mock ups. As an example of the existing facilities that can serve R&D needs in the area of MHD Thermofluids is the MaPLE (Magnetohydrodynamic PbLi Experiment) loop at UCLA [36].

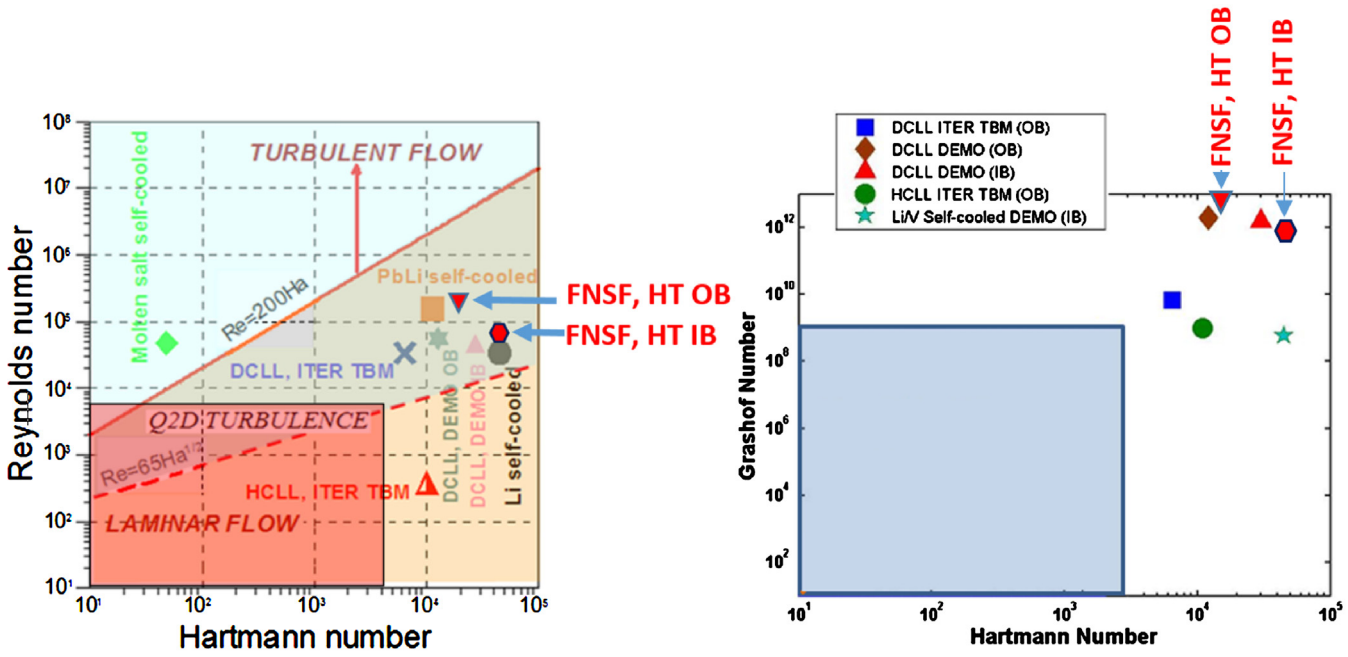

Fig. 7. Hartmann – Reynolds number (left) and Hartmann – Grashof number (right) diagram can be used to predict flow regimes in liquid-breeder blankets, including HCLL (ITER TBM), DCLL (ITER TBM and DEMO), Li/V self-cooled, PbLi self-cooled and molten salt self-cooled blankets. In the lower, middle and upper areas on the Ha-Re diagram, blanket flows are seen to be laminar, Q2D turbulent and 3D turbulent, correspondingly. Rectangular areas in the left-bottom corner of the diagrams show highest parameters in the current computations [35].

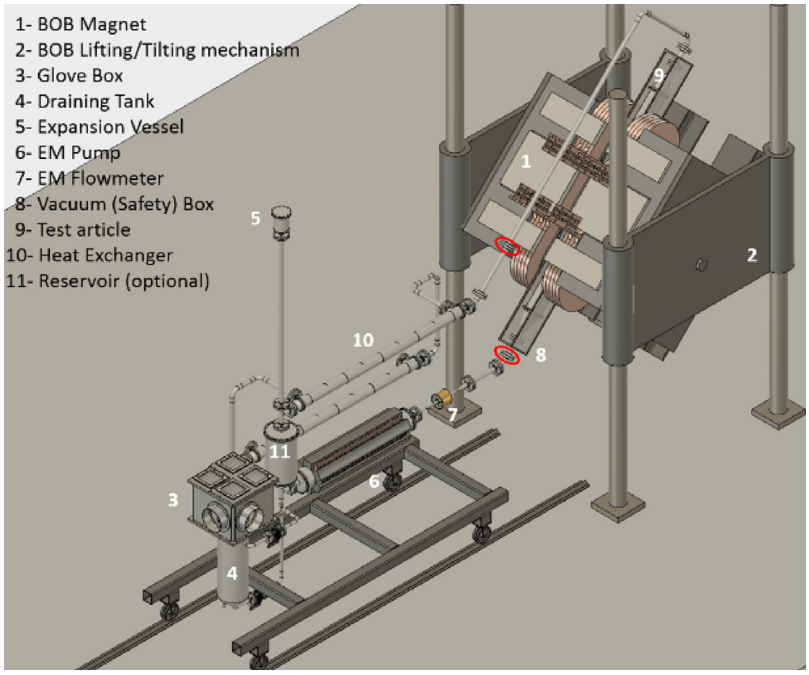

Fig. 8. Schematic of the MaPLE loop and magnet system at UCLA after the upgrade.

This facility has been under operation since 2011. The key component of the facility is a resistive water-cooled magnet (currently in the horizontal position) to study effects of a strong (up to 2 T) magnetic field on PbLi flows in a large magnet air-gap of 0.8 m x 0.15 m x 0.15 m. To significantly enhance experimental capabilities, the facility is currently under a major upgrade to allow for new experiments on multiple-effect phenomena in PbLi MHD flows. The upgrades include: (1) a new magnet lift/tilt system that would provide flexible orientation of the 20-ton electromagnet and the experimental test-section from horizontal to vertical, and (2) higher heating/cooling capabilities to inject/remove up to 70 kW of heating power (Fig. 8). These new added features would allow for experiments with dominating buoyancy effects at a maximum Grashof number of 10^9 and a maximum Hartmann number of 1500 at elevated PbLi temperatures up to 500 °C. After about five years of experiments, the facility needs to be upgraded again to replace the existing magnet with a stronger (up to 4–5 T), larger space magnet. Three groups of experiments have been identified in the upgraded MaPLE as a part of DCLL blanket collaboration between the UCLA and EUROfusion, including: (1) mixed-convection flows

for various flow orientations with respect to gravity, (2) MHD flows with electro-insulating FCIs, and (3) testing of DCLL blanket subcomponents. Detailed experimental planning is underway using similarity theory and 2-D and 3-D computations with HIMAG, COMSOL and UCLA research codes [29].

5. Concluding remarks

One of the most important results of this study is a new accurate formula for calculating the MHD pressure drop for complex 3D MHD flows in a manifold. Using this formula, along with other computational and analytical tools, resulted in accurate predictions of the MHD pressure drop for two proposed modifications of the DCLL blanket. The HT version that uses SiC FCI was demonstrated to have an acceptable MHD pressure drop. However, the analysis for the LT blanket suggests an unacceptably high MHD pressure drop of more than 5 and 14 MPa for IB and OB blankets correspondingly. The main causes of such high pressure losses in the LT DCLL blanket are higher PbLi velocities and the use of a less effective sandwich FCI compared to a SiC FCI. Although some reduction of the MHD pressure drop via further blanket optimizations seems to be possible, such a reduction would not be sufficient to satisfy the allowable pressure drop limits. Therefore, the implementation of the LT blanket in FNSF would require operating the reactor at a significantly lower power. Along with the pressure drop analysis, this study also includes a similarity analysis for the PbLi flows and preliminary plans for the pre-FNSF R&D in the area of MHD Thermofluids. The similarity analysis shows that the key dimensionless parameters in the FNSF are not very different from the DEMO reactor. Therefore, the most important physical processes in the PbLi flows will be similar between the FNSF and DEMO. The detailed investigation of these very important complex multiple-effect processes are, however, beyond the scope of the present FNSF project as it would require sophisticated 3D computations of MHD flows coupled with heat and mass transfer processes and dedicated experiments. The modified MaPLE facility at UCLA will provide flexible orientations of the test section with respect to gravity and high heating/cooling capabilities to enable experiments on convective MHD flows under various flow conditions for different heating schemes and flow geometries. These experiments along with the supporting modeling are anticipated to address the most urgent R&D needs that would lead to the successful development of the DCLL blanket concept for FNSF and next fusion devices.

Acknowledgements

The authors from UCLA acknowledge the support from the US Department of Energy, Office of Fusion Energy Sciences, under Grant # DE-FG02-86ER52123. We appreciate continuous discussions and valuable support over the entire course of the studies from Laila El-Guebaly and Edward Marriott from the University of Wisconsin.

References

[1] M. Abdou, S. Berk, A. Ying, M. Peng, S. Malang, E. Proust, et al., Results of an international study on a high-volume plasma-based neutron source for fusion blanket development, Fusion Technol. 29 (1996) 1–57.
[2] C.E. Kessel, J.P. Blanchard, A. Davis, L. El-Guebaly, N. Ghoniem, P.W. Humrickhouse, et al., The fusion nuclear science facility, the critical step in the pathway to fusion energy, Fusion Sci. Technol. 68 (2015) 225–236.
[3] S. Malang, K. Schleisiek (Editors), Dual Coolant Blanket Concept, Kernforschugszentrum Karlsruhe, Karlsruhe K fK, 1994, 5424.
[4] P. Norajitra, L. Buehler, U. Fischer, K. Kleefeldt, S. Malang, J. Reimann, et al., The Second Advanced Lead Lithium Blanket Concept using ODS Steel as Structural Material and SiC/SiC Flow Channel Insert as Electrical and Thermal Insulators, Kernforschugszentrum Karlsruhe GmbH, Karlsruhe FZKA, 1999, 6385.
[5] P. Norajitra, L. Buehler, A. Buenaventura, E. Diegele, U. Fischer, S. Gordeev, et al., Conceptual Design of the Dual-Coolant Blanket, Kernforschugszentrum Karlsruhe GmbH, Karlsruhe FZKA, 2003, 6780.
[6] P. Norajitra, L. Bühler, U. Fischer, S. Gordeev, S. Malang, G. Reimann, Conceptual design of the dual-coolant blanket in the frame of the EU power plant conceptual study, Fusion Eng. Des. 69 (2003) 669–673.
[7] M.S. Tillack, X.R. Wang, J. Pulsifer, S. Malang, D.K. Sze, M. Billone, I. Sviatoslavsky, the ARIES Team, Fusion power core engineering for the ARIES-ST power plant, Fusion Eng. Des. 65 (2003) 215–261.
[8] M.S. Tillack, S. Malang, High performance PbLi blanket, San Diego, California, Oct. 6–10, in: Proc.17th IEE/NPSS Symposium on Fusion Engineering, vol. 2, 1997, pp. 1000–1004.
[9] A.R. Raffray, L. El-Guebaly, S. Malang, X.R. Wang, L. Bromberg, T. Ihli, B. Merrill, L. Waganer, the ARIES-CS Team, Engineering design and analysis of the ARIES-CS power plant, Fusion Sci. Technol. 54 (2008) 725–746.
[10] C.P.C. Wong, S. Malang, M. Sawan, M. Dagher, S. Smolentsev, B. Merrill, et al., An overview of dual coolant Pb-17Li breeder first wall and blanket concept development for the US ITER-TBM design, Fusion. Eng. Des. 81 (2006) 461–467.
[11] C.P.C. Wong, M. Abdou, M. Dagher, Y. Katoh, R.J. Kurtz, S. Malang, et al., An overview of the US DCLL ITER-TBM program, Fusion. Eng. Des. 85 (2010) 1129–1132.
[12] J. Li, Y. Wu, S. Zheng, Preliminary neutronics design of the dual-cooled lithium lead blanket for FDS-II, in: Proc. 23rd Symposium on Fusion Technology, Venice, Italy, Sep. 20–24, 2004.
[13] H. Wang, Y. Wu, W. Wang, Preliminary thermal hydraulics design of the dual-cooled lithium lead blanket for FDS-II, in: Proc. 23rd Symposium on Fusion Technology, Venice, Italy, Sep. 20–24, 2004.
[14] Y. Wu, the FDS Team Design status and development strategy of China liquid lithium-lead blankets and related material technology, J. Nuclear Materials 367-370 (2007) 1410–1415.
[15] D. Rapisarda, I. Fernandez, I. Palermo, M. Gonzalez, C. Moreno, et al., Conceptual design of the EU-DEMO dual coolant lithium lead equatorial module, IEEE Transactions of Plasma Science 44 (2016) 1603–1612.
[16] A.R. Raffray, R. Jones, G. Aiello, M. Billone, L. Giancarli, H. Golfier, et al., Design and material issues for high performance SiCf/SiC-based fusion power cores, Fusion Eng Des. 55 (2001) 55–95.
[17] S. Sharafat, A. Aoyama, N. Morley, S. Smolentsev, Y. Katoh, B. Williams, N. Ghoniem, Development status of a SiC-foam based flow channel insert for a U.S.-ITER DCLL TBM, Fusion Sci Technol. 56 (2009) 883–891.
[18] S. Malang, M. Tillack, C.P.C. Wong, N. Morley, S. Smolentsev, Development of the lead lithium (DCLL) blanket concept, Fusion Sci. Technol. 60 (2011) 249–256.
[19] S. Smolentsev, C. Wong, S. Malang, M. Dagher, M. Abdou, MHD considerations for the DCLL inboard blanket and access ducts, Fusion Eng. Des. 85 (2010) 1007–1011.
[20] S. Smolentsev, N. Morley, M. Abdou, Code development for analysis of MHD pressure drop reduction in a liquid metal blanket using insulation technique based on a fully developed flow model, Fusion Eng. Des. 73 (2005) 83–93.
[21] S. Smolentsev, M. Abdou, N.B. Morley, M. Sawan, S. Malang, C. Wong, Numerical analysis of MHD flow and heat transfer in a poloidal channel of the DCLL blanket with a SiCf/SiC flow channel insert, Fusion Eng. Des. 81 (2006) 549–553.
[22] S. Smolentsev, N. Vetcha, M. Abdou, Effect of a magnetic field on stability and transitions in liquid breeder flows in a blanket, Fusion Eng. Des. (2013) 607–610.
[23] U. Burr, L. Barleon, U. Müller, A. Tsinober, Turbulent transport of momentum and heat in magnetohydrodynamic rectangular duct flow with strong sidewall jets, J. Fluid Mech. 406 (2000) 247–279.
[24] D.L. Smith, et al., Argonne National Laboratory, 1984, FPP-84-1.
[25] Y. Huang, N. Ghoniem, M. Tillack, J. Blanchard, L. El-Guebaly, C. Kessel, Multiphysics modeling of the FW/Blanket of the U.S. Fusion Nuclear Science Facility (FNSF), Fusion Eng. Des. 135 (2018) 279–289.
[26] S. Smolentsev, N.B. Morley, C. Wong, M. Abdou, MHD and heat transfer considerations for the US DCLL blanket for DEMO and ITER TBM, Fusion Eng Des. 83 (2008) 1788–1791.
[27] S. Smolentsev, N.B. Morley, M.A. Abdou, S. Malang, Dual-coolant lead–lithium (DCLL) blanket status and R&D needs, Fusion Eng. Des. 100 (2015) 44–54.
[28] P. Norajitra, L. Bühler, A. Buenaventura, E. Diegele, U. Fisher, S. Gordeev, et al., Conceptual Design of the Dual-Coolant Blanket within the Framework of the EU Power Plant Conceptual Study (TW2-TPR-PPCS12). Final Report FZKA 6780, Forschungszentrum Karlsruhe GmbH, 2003.
[29] S. Smolentsev, M. Abdou, C. Courtessole, G. Pulugundla, F.-C. Li, N. Morley, et al., Review of recent MHD activities for liquid metal blankets in the US, Magnetohydrodynamics 53 (2017) 411–422.
[30] U. Müller, L. Bühler, Magnetofluiddynamics in Channels and Containers, Springer, Berlin, 2001.
[31] K. Messadek, M. Abdou, Experimental study of MHD flows in a prototypic inlet manifold section of the DCLL test blanket module, Magnetohydrodynamics 45 (2009) 233–238.
[32] G. Pulugundla, S. Smolentsev, T. Rhodes, C. Kawczynski, M. Abdou, Transition to a quasi-fully-developed MHD flow in an electrically conducting pipe under a transverse non-uniform magnetic field, Fusion Sci. Technol. 68 (2015) 684–689.

[33] S. Smolentsev, M. Abdou, N.B. Morley, S. Malang, C. Kessel, R&D needs and approach to measure progress for liquid metal blankets and systems on the pathway from present experimental facilities to FNSF, Fusion Sci. Technol. 68 (2015) 245–250.
[34] M. Abdou, N.B. Morley, S. Smolentsev, A. Ying, S. Malang, A. Rowcliffe, M. Ulrickson, Blanket/first wall challenges and required R&D on the pathway to DEMO, Fusion Eng. Des. 100 (2015) 2–43.
[35] S. Smolentsev, S. Badia, R. Bhattacharyay, L. Bühler, L. Chen, Q. Huang, et al., An approach to verification and validation of MHD codes for fusion applications, Fusion Eng Des. 100 (2015) 65–72.
[36] S. Smolentsev, F.-C. Li, N. Morley, Y. Ueki, M. Abdou, T. Sketchley, Construction and initial operation of MHD PbLi facility at UCLA, Fusion Eng. Des. 88 (2013) 317–326.